

Longitudinal investigation of diffuse hemorrhagic lesions using Quantitative Susceptibility Mapping (QSM)

Andreas Petrovic¹, Ferdinand Schweser², Andreas Deistung², Eva Scheurer¹, and Jürgen R. Reichenbach²

¹Ludwig Boltzmann Institute for Clinical-Forensic Imaging, Graz, Austria, ²Medical Physics Group, Institute of Diagnostic and Interventional Radiology I, Jena University Hospital – Friedrich Schiller University Jena, Jena, Germany

Target Audience - Researchers and clinicians interested in assessing changes in soft tissue hemorrhage over time based on magnetic susceptibility changes.

Purpose - Characterization of hemorrhagic lesions is important in both, clinical and forensic medicine: While in clinical medicine the age of a brain hemorrhage may directly influence treatment strategy, in forensic medicine subcutaneous (s.c.) hemorrhages can provide important information to reconstruct the sequence of violent events. It is known that the magnetism of the iron in hemoglobin (Fe^{2+}) depends on its oxygenation state and becomes more paramagnetic with increasing deoxygenation¹. This causes magnetic field perturbations, which in turn result in T_2 shortening (due to the self diffusion of spins). For example, T_2 -relaxation times decrease with time in both, intra-cranial hemorrhages² and *in vitro* blood samples³, which may be explained by the increasing deoxygenation of the blood. Dating of hemorrhagic lesions, however, is still a largely unsolved problem⁴, and little is known about the changes of subcutaneous hemorrhages over time in MRI. The transformation from oxygenated to deoxygenated blood may be assessed non-invasively based on magnetic susceptibility obtained by the quantitative susceptibility mapping (QSM)⁵ technique. In this contribution, we applied QSM *in vivo* to yield further insight into the magnetic susceptibility changes of subcutaneous hemorrhages.

Methods – *Data acquisition*: Six healthy volunteers (3 m, 3 f, age 25.5-27 years, informed written consent) were injected 4 ml of their own venous blood into the s.c. fatty tissue of the thigh to create an artificial s.c. hemorrhage (approved by the local ethics committee). Blood was injected directly after it was taken from the antecubital vein. MRI scans were conducted before, and 40 min, 3h, 24h and 3d after the injection at 3T (Tim Trio Siemens, Erlangen, Germany) in supine position using one element of the 4-channel CPC coil (Noras, Höchberg, Germany). The acquisition protocol included an isotropic (0.6 mm) multi-echo gradient-echo sequence (FLASH) with the following parameters: TE = 2.89/8.31/13.7/18.5/23.2 ms, TR/ α =40 ms/25°. For accurate repositioning of the coil the distance of the injection location from the patella was recorded. *Data processing*: The phase images of the first echo with in-phase condition (TE=13.7ms) were used for susceptibility mapping. Phase aliasing was resolved with a Fourier-domain unwrapping algorithm⁶ and background fields were suppressed with the SHARP technique⁵ (radius 5 vx; threshold 0.015; three-fold tri-linear upsampling). The resulting images were converted into susceptibility maps using the HEIDI algorithm⁷. *Data analysis*: For quantitative analysis ROIs were drawn in the muscle, fatty tissue, and in the hematoma. ROIs in the hematoma were carefully placed in central areas of the hematoma to avoid contamination from voxels which also contain fat. Since QSM provides only relative values, susceptibility differences were computed with respect to the susceptibility in muscle tissue ($\chi_{\text{muscle}}=0$). For each subject and point in time mean values were recorded. One-way ANOVA was performed to check if the measured values changed either within (i.e. with time) or between subjects. Finally, mean values within and between subjects, and an overall average were computed.

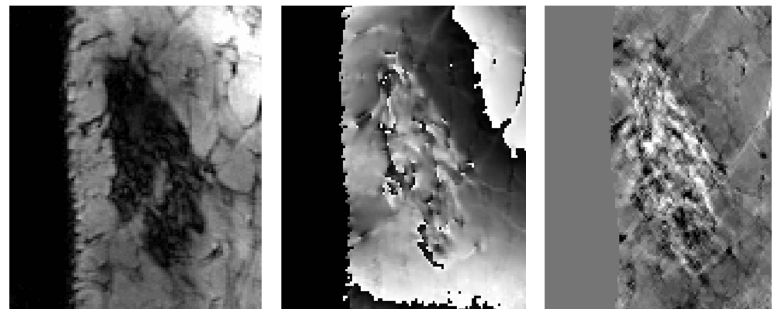


Fig. 1: Example of a fresh (40 min) artificial s.c. hematoma in MRI. Magnitude image (left), raw (wrapped) phase image (middle; TE=13.7 ms), and quantitative susceptibility map (right; from black to white: -0.4 ppm to 0.45 ppm).

Results - Figure 1 illustrates a magnitude image, phase image, and the corresponding susceptibility map of a fresh artificial s.c. hematoma. Due to substantial spin dephasing the hemorrhagic region was hypointense in the magnitude image (Fig. 1-left). In the phase image the hematoma was discernible as a hyperintense region superimposed by phase wraps (Fig. 1-middle). Compared to the magnitude image, the susceptibility maps demonstrated increased heterogeneity inside the hematomas while the surrounding fatty tissue and muscle were rather homogeneous (Fig. 1-right). The susceptibility of the hematoma was increased compared to the surrounding fatty tissue. The mean susceptibility differences of the hematomas and of fat relative to the muscle were on average $0.28 \text{ ppm} \pm 0.03 \text{ ppm}$ and $0.01 \text{ ppm} \pm 0.06 \text{ ppm}$, respectively, for all subjects and time points (table 1). Susceptibility values of both, hematomas ($p<0.05$) and fat ($p<0.01$) varied significantly between the volunteers. However, susceptibility of both, hematomas ($p=0.82$) and fat ($p=0.53$) did not change significantly during the three days of examination within volunteers.

Discussion - In the present study the expected increase of magnetic susceptibility in hematomas with time was not observed. This finding may be explained by a rather fast deoxygenation of the blood in the s.c. tissue, so that at the time of the first measurement (40 minutes after the injection) blood had already reached its maximum deoxygenation. A rough theoretical estimation shows that this explanation is in accordance with the measured susceptibility values: using the magnetic susceptibility value of fat from the literature, $\chi_{\text{Fat}} = -8.44 \text{ ppm}$ ^{8,9}, and considering that the measured susceptibility difference between fat and muscle (reference region) is negligible, the absolute average susceptibility of the hematoma may be estimated as $\chi_{\text{blood}} = -8.44 \text{ ppm} + 0.28 \text{ ppm} = -8.16 \text{ ppm}$. According to the relation between blood's magnetic susceptibility and oxygenation $\chi_{\text{Blood}}(\text{Hct}, Y) = \chi_{\text{rbc,ox}} + \text{Hct} (1-Y) \Delta\chi_{\text{do}}$ this corresponds to an oxygen saturation of the hematoma of $Y=7\%$, which is almost fully deoxygenated (assumed hematocrit (Hct) of 0.45 and the susceptibility difference between fully oxygenated and deoxygenated blood $\Delta\chi_{\text{do}} = 2.49 \text{ ppm}$ ^{10,11}). Another possible explanation for the nearly constant susceptibility values over time is the resorption of the hematoma involving on one hand an increase of the Hct associated with an increase of susceptibility, and on the other hand the recurrence of fatty tissue with a decrease of susceptibility, a process that was evident in additional data such as fat and water images (not shown).

Table 1: Measured susceptibility values for blood and fat (relative to muscle tissue) for all volunteers (V.) (Mean values within χ_w and between χ_B volunteers)

V.	χ_{Blood} in ppm					χ_{fat} in ppm				
	40 min	3h	24h	3d	Mean χ_w	40 min	3h	24h	3d	Mean χ_w
1	0.32	0.35	0.34	0.35	0.34	0.00	0.04	0.04	0.04	0.03
2	0.30	0.25	0.21	0.25	0.25	0.05	0.02	-0.04	-0.02	0.00
3	0.25	0.28	0.28	0.27	0.27	-0.01	0.00	-0.01	-0.00	0.00
4	0.35	n.a.	0.24	n.a.	0.30	0.13	n.a.	0.07	n.a.	0.10
5	0.26	0.21	0.31	0.24	0.25	0.04	0.00	-0.01	-0.01	0.01
6	0.28	0.29	0.26	0.24	0.27	-0.02	-0.03	-0.05	-0.04	-0.04
M. χ_B	0.29	0.27	0.27	0.27	0.28 ± 0.03	0.03	0.01	0.00	0.00	0.01 ± 0.06

Conclusion – The magnetic susceptibility of s.c. hemorrhage does not change within a temporal interval from 40 minutes to three days. Further research is required to elucidate the biophysical explanation of this finding.

References – 1. Ogawa S et al., 1990. *Proc Natl Acad Sci U S A*. 87:9868–72. 2. Bradley, Jr, WG, 1993. *Radiology*. 189:15-26. 3. Petrovic A et al, 2012. *Proc. Intl. Soc. Mag. Reson. Med*. 20. 1441. 4. Langlois NEI, 2007. *Forensic Sci Med Pathol*. 3:241-251. 5. Schweser F et al, 2011. *NeuroImage*. 54(4):2789–2807. 6. Schweser F et al, 2012. *Magn Reson Med* (in press). 7. Schweser F et al, 2012. *NeuroImage*. 62(3):2083–2100. 8. Szczepaniak LS et al., 2002. *Magn Reson Med*. 610:607– 610. 9. Lide DR. 1993. Boca Raton, FL: CRC Press. 10. Plyavin' YA and Blum EY, 1983. *Magneto hydrodynamics*. 19(4):349–359. 11. Zborowski M et al., 2003. *Biophys J*. 84(4):2638–45.